Peer-reviewed version available at *Appl. Sci.* **2020**, *10*, 5656; doi:10.3390/app10165656

Article

Structural, Magnetic, and Mechanical Properties of $Nd_{16}(Fe_{76-x}Co_x)B_8$ $0 \leq x \leq 25$ Alloys

Juan Sebastián Trujillo Hernández[1,2,3*], Ahmed Talaat[4*], J. A. Tabares[1], D. Oyola Lozano[3], H. Bustos Rodriguez[3], H. Martínez Sánchez[2], and G. A. Pérez Alcázar[1]

[1] Facultad de Ciencias Naturales y Matemáticas, Universidad de Ibagué, Ibagué, Colombia.
[2] Departamento de Física, Universidad del Valle, A. A. 25360, Cali, Colombia.
[3] Departamento de Física, Universidad del Tolima, Ibagué, Tolima, Colombia.
[4] Department of Mechanical Engineering and Materials Science, University of Pittsburgh, PA 15261, USA
* Correspondence: juan.trujillo@unibague.edu.co

Featured Application: Authors are encouraged to provide a concise description of the specific application or a potential application of the work. This section is not mandatory.

Abstract: *In this work, the structural, magnetic, and mechanical properties of $Nd_{16}Fe_{76-x}Co_xB_8$ alloys varying the Co content at x = 0, 10, 20 and 25, were experimentally investigated by X-Ray Diffraction (XRD), Mössbauer Spectrometry (MS), Vibrating Sample Magnetometry (VSM) at room temperature (RT), and microhardness test were performed too. The system presents the hard $Nd_2Fe_{14}B$ and the $Nd_{1.1}Fe_4B_4$ phases for samples with x = 0 and 10. When concentration increases to x= 20 and 25, the CoO phase appears. All MS show the ferromagnetic behavior (eight sextets: sites 16k1, 16k2, 8j1, 8j2, 4c, 4e, sb) associated to the hard and soft magnetic phases, and one paramagnetic component (doublet: site d) associated to the minority $Nd_{1.1}Fe_4B_4$ phase, which was not identified by XRD. All samples are magnetically hard present a hard magnetic behavior. The increase of Co content in these samples did not improve the hard magnetic behavior, but increased the critical temperature of the system and decrease the crystallite size of the hard phase. The hysteresis loop showed that predominates the $Nd_2Fe_{14}B$ hard magnetic phase. There is a general tendency to increase microhardness with cobalt content, attributable to cobalt doping reduces the lattice parameters and porosities in the sample improving it hardness.*

Keywords: Mössbauer spectroscopy; X-ray diffraction; Vibrating sample magnetometry; NdFeB magnets

1. Introduction

NdFeB permanent magnets have been investigated since 1983 [1]–[3] and continue to be investigated nowadays [4], [5] due to their high energy density (~450 kJm^{-3}) [6] that makes them useful for different applications: acoustic transducers, air conditioning, electric bikes, wind turbines, hybrid and electric cars, hard disk drives and others [7] which are the main reason of efforts to obtain an improvement in their magnetic and physics properties. The nanocomposed permanent magnets are composed of soft (α-Fe or Fe_3B) and hard ($Nd_2Fe_{14}B$) nanocrystalline magnetic phases and they present much interest because they exhibit unusual properties such as: remanence relation (Mr/Ms) larger than 0.5 (the Stoner–Wohlfarth limitation) due the exchange coupling between these two phases[8]. Among earlier works on this nanocomposites magnet was carried out by Coehoorn, R et. al [9] that investigated $Fe_3B/Nd_2Fe_{14}B$ through of melt-spinning, showed values of 0.3 T and 93 kJm^{-3} for coercive and magnetic energy, respectively. After these works, different theoretical models [10]–[12] were proposed in order to improve our understanding of the exchange-coupled nanocomposite magnet. Many works that using it model have been carry out by thin film; for example, Cui, W et. al [13] investigated $Nd_2Fe_{14}B$/FeCo anisotropic nanocomposite films, and they have obtained values of maximum energy product between 400 and 500 kJm^{-3} through exchange-coupled. On the other hand,

Yang. F et. al [4] recently investigated the bonded magnets of NdFeB with $SrFe_{12}O_{19}$ ferrite by additive manufacturing (3D printing); for the sample with 20 wt.% of ferrite they obtained a relatively low surface roughness of ~6 μm and a tensile strength of 12 MPa. However, they obtained decrease in magnetic properties saturation magnetization (M_s), remanent magnetization (M_r), coercive field (H_c) and maximum energy product $(BH)_{max}$ with the increased content wt.% of ferrite. Other recent work in the system NdFeB using the same principle is reported in the reference [5], where the phase and hyperfine structure of melt-spun nanocrystalline $(Ce_{1-x}Nd_x)_{16}Fe_{78}B_6$ alloys are studied, they found that alloys are composed specifically by the phase $(NdCe)_2Fe_{14}B$, however phases like $(CeNd)Fe_2$ and $(CeNd)Fe_4B_4$ was also identified. The Mössbauer fitted was carry out to used six sextets and two doublet component; the average magnetic hyperfine field by Mössbauer and the magnetic properties M_s, H_c and $(BH)_{max}$ increased for the composition from x=0 to x=0.7. These properties are sensible to the type of elements of the hard [14]–[19] and soft phases [14], [20], to the grain size of the hard phase [15], [16], [21]–[24], and to the different techniques used to prepare them [25]–[36].

Considering that Co is a ferromagnetic transition metal and its atomic ratio is 1.25 Å that is comparison whit that of the Fe (1.26 Å), moreover that the Co have a tetragonal crystalline structure with uniaxial anisotropy. In this direction we are interested in study the effect of Co in the properties of $Nd_{16}Fe_{76-x}Co_xB_8$ alloys (x = 0, 10, 20, and 25) obtained through arc-furnace, and characterized by x-ray diffraction (XRD), Mossbauer spectrometry (MS), vibrating sample magnetometry (VSM), and microhardness studies.

2. Materials and Methods

Alloys of the $Nd_{16}Fe_{76-x}Co_xB_8$ (x=0, 10, 20, and 25) system were prepared by mixing and compacting high purity fine powders (>99.9%) of Fe, Nd, B and Co. These samples were prepared by arc-melting method under Ar atmosphere. Afterwards, the samples were encapsulated in evacuated quartz tubes and finally heat treated at 1073 K for 30 minutes and quenched in ice water. All the prepared samples were characterized by MS, XRD, VSM, and Microhardness studies. Mössbauer measurements were performed in a constant acceleration spectrometer at room temperature with transmission geometry using a $^{57}Co(Rh)$ source of 25 mCi. All spectra were fitted with the MOSFIT program [37] and the isomeric deviation values were referred to α-Fe. The XRD measurements were obtained by using the Cu-Kα radiation and the patterns were refined by using the GSAS program [38], which is based in the Rietvelt method combined with Fourier analysis to describe the broadening of the lines. This refinement yields the average values of the lattice parameters and of the crystallite sizes, and quantify the obtained structural phases. The behavior of the magnetization as a function of the field was studied by using the VSM of the Physics Properties Measurements System (PPMS) of the Excellence Centre for New Materials (CENM) of Universidad del Valle, Colombia. Vickers hardness tests were performed on heat-treated samples, which have been polished to a mirror finish with alumina 0.05 μm particle size. Microhardness maps were performed on a Leco AMH43 microhardness automated, on different areas of the samples, applying a load of 200 g and a holding time of 15 s.

3. Results

3.1. XRD

Figure 1 shows XRD patterns obtained for some samples with different Co concentrations. These patterns reveal that all samples present the tetragonal $Nd_2Fe_{14}B$ hard phase (space group P42/mmm) and the $Nd_{1.1}Fe_4B_4$ phase (tetragonal structure and orthorhombic space group *Pccn*) [39]–[42]. Also, the CoO phase (Wurzita structure and space group *P63mc*) for high concentrations of Co (x = 20 and 25) was detected. In Fig. 1 it can be noted how the intensity of the peaks corresponding to the $Nd_2Fe_{14}B$ phase is slightly reduced and those of the $Nd_{1.1}Fe_4B_4$ increase when Co content increases.

Rietveld refinement allowed us to determine the type of structures having these alloys. The parameter values for samples with stoichiometry $Nd_{16}Fe_{76-x}Co_xB_8$ with x = 0, 10, 20 and 25 are reported

in Table 1. These data indicate that the crystallite size for $Nd_{1.1}Fe_4B_4$ and $Nd_2Fe_{14}B$ phases are in the nanometer range, from 5 to 90 nm. Crystallite size parallel to the $Nd_{1.1}Fe_4B_4$ and $Nd_2Fe_{14}B$ phases increases with increased concentration of cobalt. It can be noted that systematically, the two phases parallel crystallite sizes are greater than the perpendicular ones, indicating that the crystallite shape is not spherical but elongated in that direction. The refinement of the mean crystallite size of the hard phase is required in order to obtain higher remanence values [43], [44] and to increase the ferromagnetic exchange coupling between the soft and hard grains [10]. The obtained values of the crystallite size indicate that these melted alloys are nanostructured.

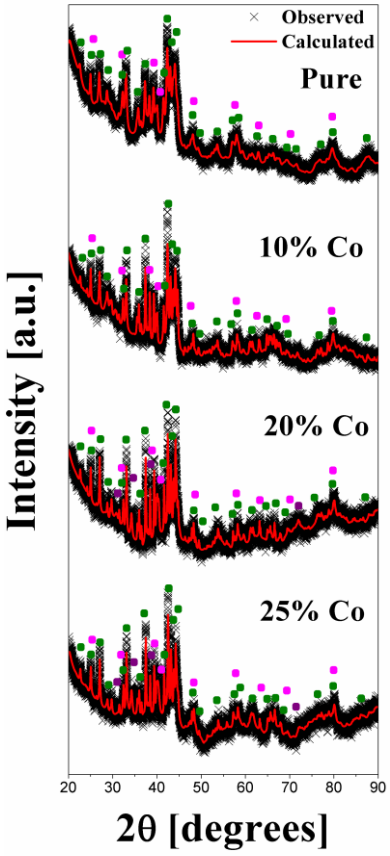

Figure 1. XRD patterns of the $Nd_{16}Fe_{76-x}Co_xB_8$ samples with x = 0, 10, 20, and 25 at room temperature, when ● $Nd_2Fe_{14}B$, ● $Nd_{1.1}Fe_4B_4$ and ● CoO.

Table 1. Structural parameters of the $Nd_{16}Fe_{76-x}Co_xB_8$ samples with x = 0, 10, 20, and 25

PHASE	$Nd_2Fe_{14}B$					
%Co	%Phase ± 0.3	*a*[Å] ± .001	*c*[Å] ± .001	Vol. [Å^3] ± 0.6	Φ ⊥ [nm] ± 1.7	Φ // [nm] ± 1.7
0	83.8	8.814	12.210	948.7	19.3	25.0
10	68.8	8.799	12.174	942.7	32.4	48.3
20	60.5	8.768	12.138	933.2	55.0	94.8
25	63.5	8.762	12.136	931.9	44.5	81.0
PHASE	$Nd_{1.1}Fe_4B_4$					
%Co	%Phase ± 0.3	*a*[Å] ± .001	*c*[Å] ± .001	Vol. [Å^3] ± 0.6	Φ ⊥ [nm] ± 1.0	Φ // [nm] ± 1.0
0	15.9	7.113	35.632	1802.9	64.7	5.2

Preprints (www.preprints.org) | NOT PEER-REVIEWED | Posted: 25 July 2020 doi:10.20944/preprints202007.0612.v1

Peer-reviewed version available at Appl. Sci. 2020, 10, 5656; doi:10.3390/app10165656

10	31.2	7.096	35.090	1769.9	85.7	10.7
20	33.1	7.108	35.126	1761.1	52.6	3.8
25	28.7	7.100	34.993	1764.6	32.3	15.5
PHASE			***CoO***			
%Co	**%Phase ± 0.4**	***a*[Å] ± 0.001**	***c*[Å] ± .001**	**Vol. [Å^3] ± 0.2**	**Φ ⊥ [nm] ± 2.0**	**Φ // [nm] ± 2.0**
0	--	--		--	--	--
10	--	--		--	--	--
20	6.4	3.185	5.249	46.1	19.0	22.6
25	7.7	3.240	5.234	47.61	38.8	25.3

In Table 1 the quantitative evolution with the Co content of the weight fraction of the different obtained phases. It can be noted that the Co also decreases the stability of the hard phase and the decomposition of this phase conduces to the increment of the $Nd_{1.1}Fe_4B_4$ phase.

Figure 2a and 2b show the behavior of the lattice parameters with respect to the cobalt concentration of the $Nd_2Fe_{14}B$ and $Nd_{1.1}Fe_4B_4$ phases for all samples. It is observed for x = 0, 10, 20 and 25, lattice parameters *a* and *c* of $Nd_2Fe_{14}B$ and $Nd_{1.1}Fe_4B_4$ phases, decrease considerably with the variation of the concentration of cobalt. This behavior is a consequence of the substitution of Fe by Co atoms, which has an atomic radius (1.25 Å) less than the atomic radius of iron (1.26 Å) and make the lattice to reduce. These parameters are consistent with those reported in the literature [45], [46].

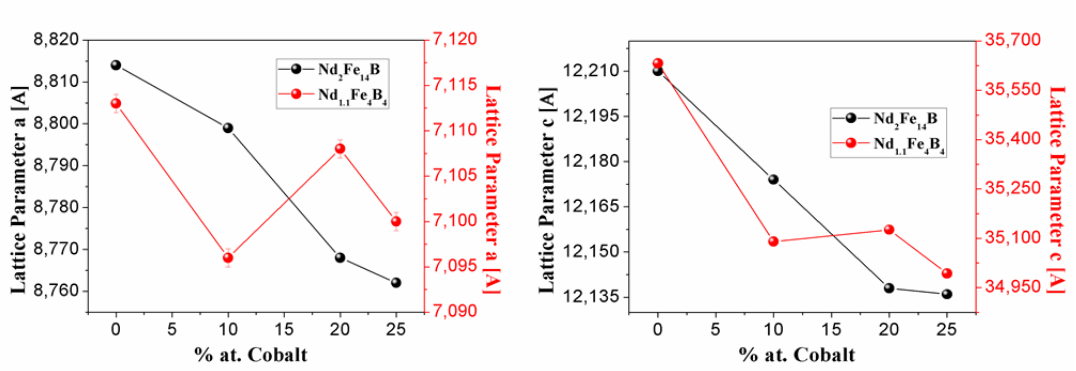

Figure 2. a left) Lattice parameter *a* as a function of Co content of the $Nd_2Fe_{14}B$ and $Nd_{1.1}Fe_4B_4$ phases, and b right) Lattice parameter *c* as a function of Co content of the $Nd_2Fe_{14}B$ and $Nd_{1.1}Fe_4B_4$ phases.

3.2. Mossbauer Results

The Mössbauer spectra of $Nd_{16}Fe_{76-x}Co_xB_8$ (x = 0, 10, 20 and 25) samples, collected at RT, are shown in Fig. 3. To fit these spectra, it was necessary several subspectra, which were associated with the $Nd_2Fe_{14}B$, α-Fe and $Nd_{1.1}Fe_4B_4$ phases. The last one was not identified by XRD. Seven sextets were used to fit the magnetic part of the spectra, six of them corresponding to those reported for the hard phase ($16k_1$, $16k_2$, $8j_1$, $8j_2$, 4c and 4e) and the other corresponds to the α-Fe phase (s^b) reported by Hernandez *et al*. [47]–[49]. As can be observed, the Mössbauer spectrum of the sample with x = 0 is the typical one of the $Nd_2Fe_{14}B$ phase [8]. It was necessary to add a small doublet (site d) in order to obtain the best fit, and this was attributed to the paramagnetic $Nd_{1.1}Fe_4B_4$ phase [47]. The Mössbauer parameters, like a hyperfine magnetic field (H_{hf}), isomer shift (IS), quadrupole splitting (QS), and area of each subspectra, are listed in Table 2. The value of line width (Γ) takes values of 0.33 mm/s for all sextets and 0.40 mm/s for doublet; attributable to a degree of disorder of the samples.

Preprints (www.preprints.org) | NOT PEER-REVIEWED | Posted: 25 July 2020 doi:10.20944/preprints202007.0612.v1

Peer-reviewed version available at Appl. Sci. 2020, 10, 5656; doi:10.3390/app10165656

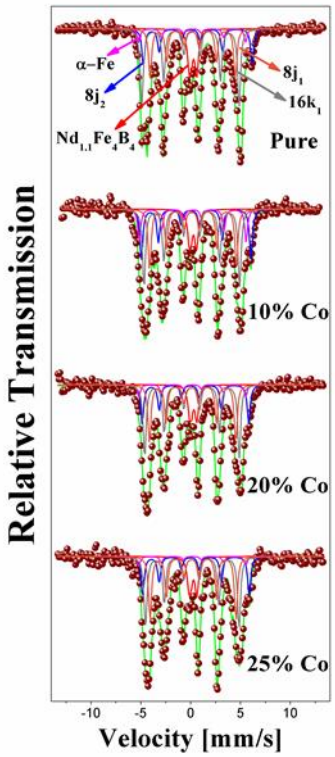

Figure 3. Mössbauer spectra of the $Nd_{16}Fe_{76-x}Co_xB_8$ samples with x = 0, 10, 20, and 25 at room temperature.

Table 2. Hyperfine parameters: hyperfine field H_{hf}, relative area, sites of the Mössbauer spectra of the $Nd_{16}Fe_{76-x}Co_xB_8$ samples with x = 0, 10, 20, and 25.

% at. Co	Phase	Site	[%]Area ±0.1	H_{hf}[T] ±0.1
x= 0 ($N_{16}Fe_{76}B_8$)	$Nd_{1.1}Fe_4B_4$	d	8,4	0
	αFe	S^b	4,0	330
	$Nd_2Fe_{14}B$	$16k_1$	14,3	292,4
		$16k_2$	15,7	310,5
		$8j_1$	13,2	274,7
		$8j_2$	11,0	344,9
		4c	23,9	283,7
		4e	9,4	242,3
% at. Co	**Phase**	**Site**	**[%]Area ±0.1**	**H_{hf}[T] ±0.1**
x= 10 ($N_{16}Fe_{66}Co_{10}B_8$)	$Nd_{1.1}Fe_4B_4$	d	6,4	0
	αFe	S^b	5,0	330
	$Nd_2Fe_{14}B$	$16k_1$	20,9	296,8
		$16k_2$	7,9	327,1
		$8j_1$	16,7	268,7
		$8j_2$	10,8	350,5
		4c	22,5	296,4
		4e	9,7	242,8
% at. Co	**Phase**	**Site**	**[%]Area ±0.1**	**H_{hf}[T] ±0.1**
x= 20 ($N_{16}Fe_{56}Co_{20}B_8$)	$Nd_{1.1}Fe_4B_4$	d	6,7	0
	αFe	S^b	3,5	330

	$Nd_2Fe_{14}B$	$16k_1$	16,1	291,1
		$16k_2$	17,6	305,2
		$8j_1$	16,7	264,5
		$8j_2$	11,9	330,6
		4c	16,8	280,1
		4e	10,7	242,5
% at. Co	**Phase**	**Site**	**[%]Area ±0.1**	**H_{hf}[T] ±0.1**
x= 25 $(N_{16}Fe_{51}Co_{25}B_8)$	$Nd_{1.1}Fe_4B_4$	d	6,9	0
	αFe	s^b	3,1	330
	$Nd_2Fe_{14}B$	$16k_1$	21,3	292,5
		$16k_2$	15,7	294,6
		$8j_1$	14,4	261,8
		$8j_2$	11,4	329,6
		4c	19,0	265,7
		4e	8,3	229,9

Fig. 4a shows the variation of the hyperfine field, H_{hf}, of the different inequivalent Fe sites in the $Nd_2Fe_{14}B$ hard magnetic phase as a function of Co content. It can be noted that the hyperfine field of the different sites has a tendency to decrease. This decrease is mainly due to the cobalt has a magnetic moment (1.71μB/atom) less than the magnetic moment of iron (2.22μB/atom), and this result suggests that cobalt atoms are entering within the lattice of $Nd_2Fe_{14}B$. But for site 4c the higher decreasing of hyperfine field with the cobalt concentration occurs; this result indicates that the cobalt atoms have a preference for substituting iron atoms at those sites. These results agree with Liao *et al.* [49].

In Fig. 4b, the results are also consistent, which shows a high decrease in the relative area 4c, confirming the preference of cobalt atoms replacing iron atoms at these sites, comparing 8j1, 8j2, 16k1, 16k2 and 4e sites, which have a tendency to increase their relative area; then the cobalt does not replace iron atoms of these sites and ferromagnetism of these sites increases.

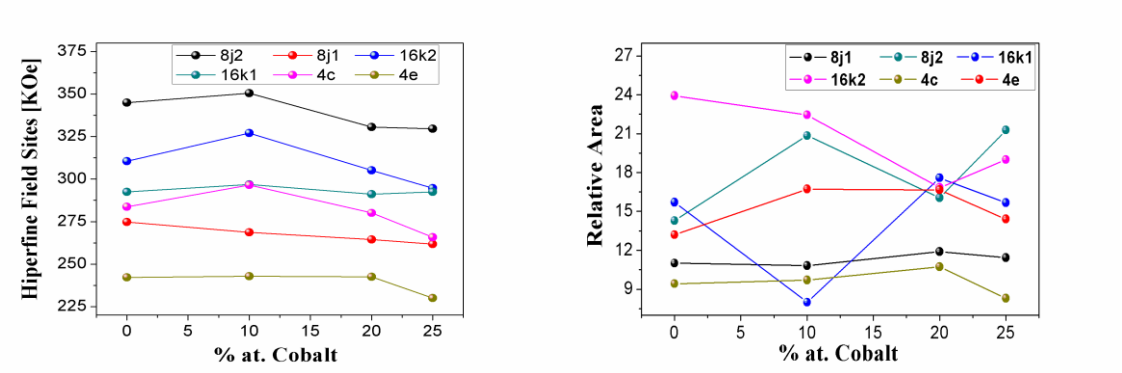

Figure 4. a left) Hyperfine field of Fe sites (16k1, 16k2, 8j1, 8j2, 4c and 4e) of the hard magnetic phase Nd2Fe14B as a function of Co content, and b right) Relative area of Fe sites (16k1, 16k2, 8j1, 8j2, 4c and 4e) of the hard magnetic phase Nd2Fe14B as a function of Co content.

Figure 5a. It can be observed that there is a general tendency of the mean hyperfine field (MHF) to decrease as cobalt content increases. Fig. 5b shows the behavior of the relative area of the site d ($Nd_{1.1}Fe_4B_4$) and site s^b (α-Fe) relative to Co content. A behavior to diminish the relative area of the site d ($Nd_{1.1}Fe_4B_4$), suggests that substituting iron atoms by cobalt atoms destabilizes $Nd_{1.1}Fe_4B_4$ phase. Besides, the Fig.5b shows that the relative area of the α-Fe phase decreases with the cobalt content. These results indicate that the cobalt atom diffuse into the structure of $Nd_2Fe_{14}B$ substituting and expels iron atoms, producing Fe segregated.

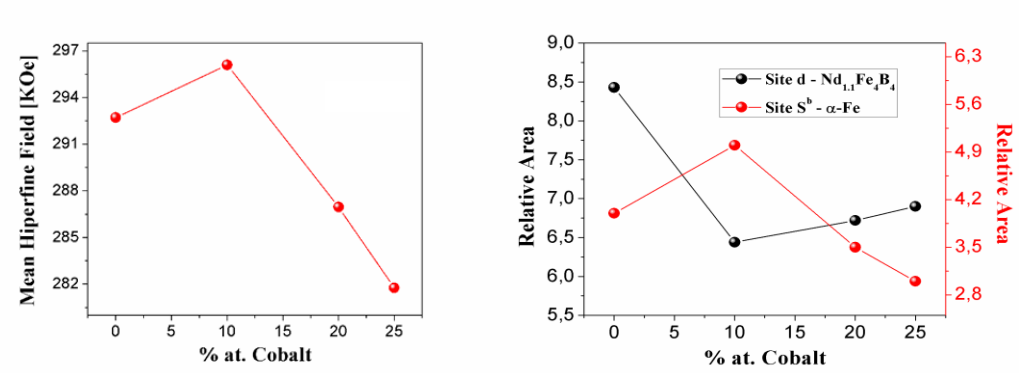

Figure 5. a left) Mean hyperfine field of the $Nd_{16}Fe_{76-x}Co_xB_8$ samples with x = 0, 10, 20, and 25 at room temperature, and b right) Variation of relative spectral area of the sites α-Fe (S^b) and $Nd_{1.1}Fe_4B_4$ (d) as a function of Co content.

3.3. Magnetic properties

Figure 6 shows the hysteresis loops for the alloys with x = 0, 10, 20 and 25. In all samples predominates the Nd2Fe14B hard magnetic phase. But the addition of cobalt reduces the size and width of the hysteresis loop, especially for x = 25. These samples reach the saturation magnetization when the fields are higher than 2.5 T. On the other hand, the values (see Table 4) of the coercive field H_c decrease with the increase of Co content, as shown in Fig. 7a. Despite such decrease in coercivity, all samples are still displaying a hard-magnetic character.

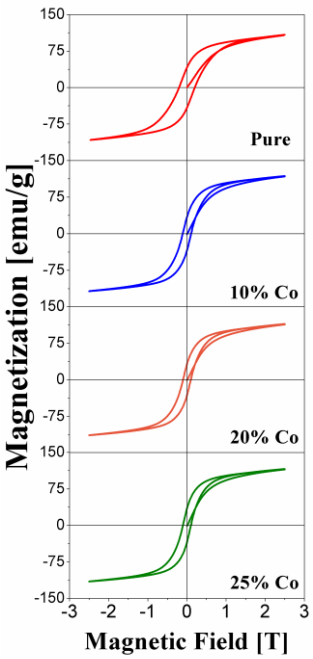

Figure 6. Hysteresis loop of the $Nd_{16}Fe_{76-x}Co_xB_8$ samples with x = 0, 10, 20, and 25 at room temperature.

Fig. 7b shows the behavior of the saturation magnetization M_s and of the remanent magnetization M_r with the concentration of cobalt is presented. It can be concluded that increasing the concentration of cobalt increases the saturation magnetization and decreases the remanent magnetization. This behavior can be explained considering that cobalt has a lower magnetic moment of iron and also stimulates the creation of only one CoO phase, and this does not limit the creation of $Nd_2Fe_{14}B$ hard magnetic phase. These results agree with those reported by Lin *et al.* [50].

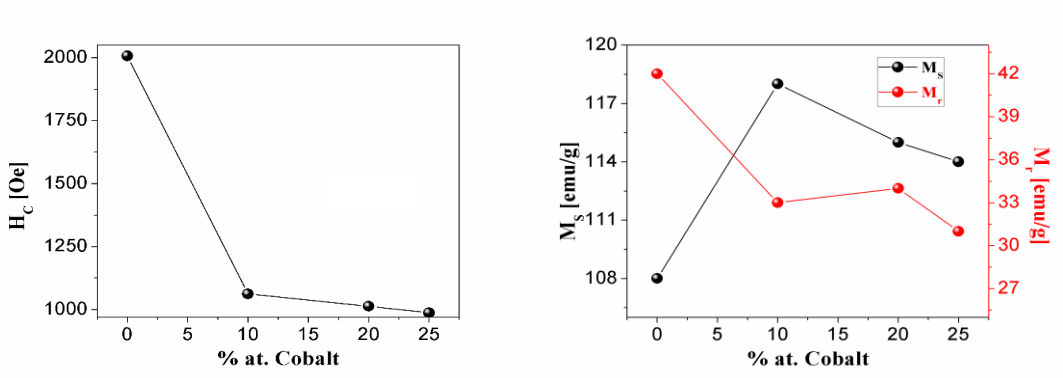

Figure 7. a left) Variation of coercive field *Hc* as a function of Co content, and b right) Variation of saturation magnetization M_s and remanent magnetization M_r as a function of Co content.

3.4. Microhardness

We carried out hardness evolution of the system $Nd_{16}Fe_{76-x}Co_xB_8$ with x = 0, 10, 20 and 25 as a function of the atomic percentage of cobalt. The microhardness values of the samples with respect to the cobalt content. Fig. 8a shows the data obtained in relation to the cobalt concentration. We can see a general tendency to increase the microhardness with the cobalt content, due to cobalt doping which reduces the lattice parameters and the porosities in the sample improving its hardness as can be appreciated in the microhardness images presented in Fig. 8b.

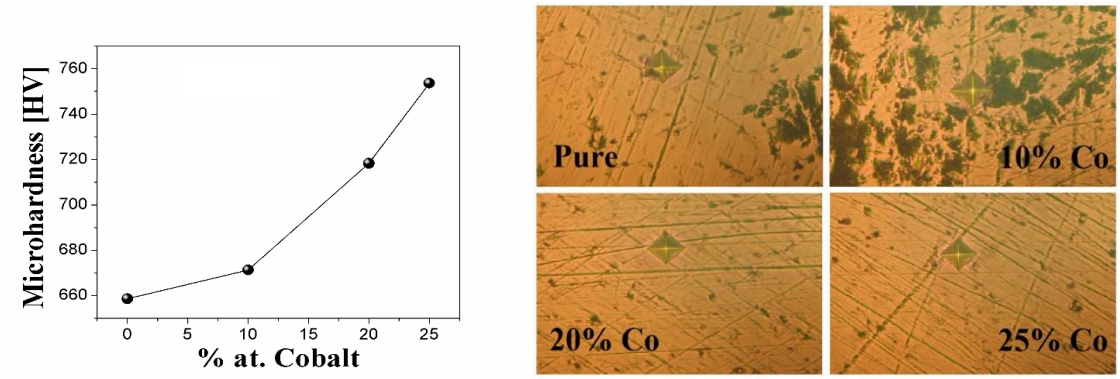

Figure 8. a left) Variation of the microhardness as a function of Co content, and b right) Images of the trace made for obtaining the microhardness at (500X) as a function of Co content.

4. Conclusions

From the results of present work, it can be concluded that the substitution of Fe by Co atoms in the $Nd_{16}Fe_{76-x}Co_xB_8$ nanocomposite alloy decreases the magnetic hard character of the system. The increase of the Co content decreases the stability of the hard phase. The hard phase decreases due the decrease of the 4c site when Co content increases. The magnetic softening of the samples is principally due to the low ferromagnetic coupling between the soft and hard phases. There is a general trend of microhardness increase with cobalt content, which is attributable to the role of cobalt doping in reducing the lattice parameters and porosities in the sample

In summary, the coupling between NdFeB and Co generates nanostructured systems that favor the formation of hard and soft magnetic phases and improves the ductility conditions which improves the magnetic and mechanical properties of exchange coupling magnets.

Author Contributions: For research articles with several authors, a short paragraph specifying their individual contributions must be provided. The following statements should be used "conceptualization, Juan Trujillo,

German Pérez, and Dagoberto Oyola.; methodology, Juan Trujillo, and Humberto Bustos.; software, Juan Trujillo, and Hugo Martinez.; validation, Juan Trujillo, German Pérez. and Dagoberto Oyola; formal analysis, Juan Trujillo, and Ahmed Talaat.; investigation, Juan Trujillo.; writing—original draft preparation, Juan Trujillo; writing—review and editing, Ahmed Talaat,; supervision, Dagoberto Oyola, and Jesus Tabares; project administration, Dagoberto Oyola, and German Pérez; funding acquisition, Dagoberto Oyola, and German Pérez.

Funding: This research was funded by COLCIENCIAS, grant number FP 44842-104-2016 and The Estancia Posdoctoral Colciencias was funded by convocatoria 811-2018.

Acknowledgments: The authors express special thanks to the Research Office of the Universidad del Tolima and COLCIENCIAS, under Contract FP 80740-415-2019, for the financing of this work.

Conflicts of Interest: The authors declare no conflict of interest

References

[1] J. J. Croat, J. F. Herbst, R. W. Lee, and F. E. Pinkerton, "High-energy product Nd-Fe-B permanent magnets," *Applied Physics Letters*, vol. 44, no. 1, 1984, doi: 10.1063/1.94584.

[2] M. Sagawa, S. Fujimura, N. Togawa, H. Yamamoto, and Y. Matsuura, "New material for permanent magnets on a base of Nd and Fe (invited)," *Journal of Applied Physics*, vol. 55, no. 6, 1984, doi: 10.1063/1.333572.

[3] G. C. Hadjipanayis, "Nanophase hard magnets," *Journal of Magnetism and Magnetic Materials*, vol. 200, no. 1–3, 1999, doi: 10.1016/S0304-8853(99)00430-8.

[4] F. Yang, X. Zhang, Z. Guo, S. Ye, Y. Sui, and A. A. Volinsky, "3D printing of NdFeB bonded magnets with SrFe12O19 addition," *Journal of Alloys and Compounds*, vol. 779, 2019, doi: 10.1016/j.jallcom.2018.11.335.

[5] L. Z. Zhao *et al.*, "Phase and Hyperfine Structures of Melt-spun Nanocrystalline (Ce1-xNdx)16Fe78B6 Alloys," *IEEE Transactions on Magnetics*, vol. 53, no. 11, 2017, doi: 10.1109/TMAG.2017.2695533.

[6] R. Madugundo, N. V. Rama Rao, A. M. Schönhöbel, D. Salazar, and A. A. El-Gendy, "Recent Developments in Nanostructured Permanent Magnet Materials and Their Processing Methods," in *Magnetic Nanostructured Materials: From Lab to Fab*, 2018.

[7] J. Fischbacher *et al.*, "Micromagnetics of rare-earth efficient permanent magnets," *Journal of Physics D: Applied Physics*, vol. 51, no. 19. 2018, doi: 10.1088/1361-6463/aab7d1.

[8] R. W. McCallum, A. M. Kadin, G. B. Clemente, and J. E. Keem, "High performance isotropic permanent magnet based on Nd-Fe-B," *Journal of Applied Physics*, vol. 61, no. 8, 1987, doi: 10.1063/1.338706.

[9] R. Coehoorn, D. B. de Mooij, J. P. W. B. Duchateau, and K. H. J. Buschow, "NOVEL PERMANENT MAGNETIC MATERIALS MADE BY RAPID QUENCHING," *Le Journal de Physique Colloques*, vol. 49, no. C8, 1988, doi: 10.1051/jphyscol:19888304.

[10] E. F. Kneller and R. Hawig, "The exchange-spring magnet: A new material principle for permanent magnets," *IEEE Transactions on Magnetics*, vol. 27, no. 4, 1991, doi: 10.1109/20.102931.

[11] E. E. Fullerton, J. S. Jiang, and S. D. Bader, "Hard/soft magnetic heterostructures: model exchange-spring magnets," *Journal of Magnetism and Magnetic Materials*, vol. 200, no. 1–3, 1999, doi: 10.1016/S0304-8853(99)00376-5.

[12] A. López-Ortega, M. Estrader, G. Salazar-Alvarez, A. G. Roca, and J. Nogués, "Applications of exchange coupled bi-magnetic hard/soft and soft/hard magnetic core/shell nanoparticles," *Physics Reports*, vol. 553. 2015, doi: 10.1016/j.physrep.2014.09.007.

[13] W. bin Cui, Y. K. Takahashi, and K. Hono, "Nd2Fe14B/FeCo anisotropic nanocomposite films with a large maximum energy product," *Advanced Materials*, vol. 24, no. 48, 2012, doi: 10.1002/adma.201202328.

[14] W. C. Chang, D. Y. Chiou, S. H. Wu, B. M. Ma, and C. O. Bounds, "High performance α-Fe/Nd2Fe14B-type nanocomposites," *Applied Physics Letters*, vol. 72, no. 1, 1998, doi: 10.1063/1.121446.

[15] X. C. Kou, M. Dahlgren, R. Grössinger, and G. Wiesinger, "Spin-reorientation transition in nano-, micro- and single-crystalline Nd2Fe14B," *Journal of Applied Physics*, vol. 81, no. 8 PART 2A, 1997, doi: 10.1063/1.364791.

[16] V. Villas-Boas, S. A. Romero, and F. P. Missell, "Flash annealing and magnetic interactions in Pr4Fe78B18," *Journal of Applied Physics*, vol. 81, no. 8, 1997, doi: 10.1063/1.364793.

[17] G. P. Wang, W. Q. Liu, Y. L. Huang, S. C. Ma, and Z. C. Zhong, "Effects of sintering temperature on the mechanical properties of sintered NdFeB permanent magnets prepared by spark plasma sintering," *Journal of Magnetism and Magnetic Materials*, vol. 349, 2014, doi: 10.1016/j.jmmm.2013.08.044.

[18] H. Z. Yan, F. Q. Kong, W. Xiong, B. Q. Li, J. Li, and L. Wang, "New La-Fe-B ternary system hydrogen storage alloys," *International Journal of Hydrogen Energy*, vol. 35, no. 11, 2010, doi: 10.1016/j.ijhydene.2010.02.127.

[19] B. Y. Hou, Z. Xu, S. Peng, C. Rong, J. P. Liu, and S. Sun, "A facile synthesis of SmCo5 magnets from core/shell Co/Sm 2O3 nanoparticles," *Advanced Materials*, vol. 19, no. 20, 2007, doi: 10.1002/adma.200700891.

[20] I. Betancourt and H. A. Davies, "Exchange coupled nanocomposite hard magnetic alloys," *Materials Science and Technology*, vol. 26, no. 1, 2010, doi: 10.1179/026708309X12548155118860.

[21] D. Oyola Lozano, L. E. Zamora, G. A. Pérez Alcázar, Y. A. Rojas, H. Bustos, and J. M. Greneche, "Magnetic and structural properties of the Nd2(Fe 100-xNbx)14B system prepared by arc melting," *Hyperfine Interactions*, vol. 169, no. 1–3, 2006, doi: 10.1007/s10751-006-9433-z.

[22] C. Y. You, Y. K. Takahashi, and K. Hono, "Fabrication and characterization of highly textured Nd-Fe-B thin film with a nanosized columnar grain structure," in *Journal of Applied Physics*, 2010, vol. 108, no. 4, doi: 10.1063/1.3474990.

[23] B. Z. Cui *et al.*, "Relation between structure and magnetic properties of Nd2(Fe, Co, Mo)14B/α-Fe nanocomposite magnets," *Journal of Alloys and Compounds*, vol. 340, no. 1–2, 2002, doi: 10.1016/S0925-8388(02)00014-2.

[24] J. A. Valcanover, C. Paduani, J. D. Ardisson, C. A. S. Pérez, and M. I. Yoshida, "Mössbauer effect and magnetization studies of Nd16Fe 76 - XRuxB8 alloys," *Acta Materialia*, vol. 53, no. 9, 2005, doi: 10.1016/j.actamat.2005.02.042.

[25] T. Fukagawa, T. Ohkubo, S. Hirosawa, and K. Hono, "Nano-sized disorders in hard magnetic grains and their influence on magnetization reversal at artificial Nd/Nd2Fe14B interfaces," *Journal of Magnetism and Magnetic Materials*, vol. 322, no. 21, 2010, doi: 10.1016/j.jmmm.2010.06.023.

[26] W. B. Cui, Y. K. Takahashi, and K. Hono, "Microstructure optimization to achieve high coercivity in anisotropic Nd-Fe-B thin films," *Acta Materialia*, vol. 59, no. 20, 2011, doi: 10.1016/j.actamat.2011.09.006.

[27] T. Saito, "Electrical resistivity and magnetic properties of Nd-Fe-B alloys produced by melt-spinning technique," *Journal of Alloys and Compounds*, vol. 505, no. 1, 2010, doi: 10.1016/j.jallcom.2010.05.175.

[28] B. M. Ma, J. W. Herchenroeder, B. Smith, M. Suda, D. Brown, and Z. Chen, "Recent development in bonded NdFeB magnets," *Journal of Magnetism and Magnetic Materials*, vol. 239, no. 1–3, 2002, doi: 10.1016/S0304-8853(01)00609-6.

[29] D. J. Keavney, E. E. Fullerton, J. E. Pearson, and S. D. Bader, "High-coercivity, c-axis oriented Nd2Fe14B films grown by molecular beam epitaxy," *Journal of Applied Physics*, vol. 81, no. 8, 1997, doi: 10.1063/1.364969.

[30] T. Nishio, S. Koyama, Y. Kasai, and V. Panchanathan, "Low rare-earth Nd–Fe–B bonded magnets with improved irreversible flux loss," *Journal of Applied Physics*, vol. 81, no. 8, 1997, doi: 10.1063/1.364971.

[31] M. R. Corfield, A. J. Williams, and I. R. Harris, "Effects of long term annealing at 1000 °C for 24 h on the microstructure and magnetic properties of Pr-Fe-B/Nd-Fe-B magnets based on Nd16Fe76B8 and Pr16Fe76B8," *Journal of Alloys and Compounds*, vol. 296, no. 1–2, 2000, doi: 10.1016/S0925-8388(99)00506-X.

[32] M. Yue, M. Tian, J. X. Zhang, D. T. Zhang, P. L. Niu, and F. Yang, "Microstructure and magnetic properties of anisotropic Nd-Fe-B magnets produced by spark plasma sintering technique," *Materials Science and Engineering B: Solid-State Materials for Advanced Technology*, vol. 131, no. 1–3, 2006, doi: 10.1016/j.mseb.2005.11.010.

[33] S. Pandian, V. Chandrasekaran, G. Markandeyulu, K. J. L. Iyer, and K. V. S. Rama Rao, "Effect of Al, Cu, Ga, Nb additions on the magnetic properties and microstructural features of sintered NdFeB," *Journal of Applied Physics*, vol. 92, no. 10, 2002, doi: 10.1063/1.1513879.

[34] Z. Wang, S. Zhou, M. Zhang, and Y. Qiao, "High-performance α-Fe/Pr2Fe14B-type nanocomposite magnets produced by hot compaction under high pressure," *Journal of Applied Physics*, vol. 88, no. 1, 2000, doi: 10.1063/1.373701.

[35] V. Pop, S. Gutoiu, E. Dorolti, O. Isnard, and I. Chicina, "The influence of short time heat treatment on the structural and magnetic behaviour of Nd 2 Fe 14 B/α-Fe nanocomposite obtained by mechanical milling," *Journal of Alloys and Compounds*, vol. 509, no. 41, 2011, doi: 10.1016/j.jallcom.2011.08.002.

[36] V. Neu and L. Schultz, "Two-phase high-performance Nd-Fe-B powders prepared by mechanical milling," *Journal of Applied Physics*, vol. 90, no. 3, 2001, doi: 10.1063/1.1380223.

[37] F. Varret and J. Teillet, "Unpublished MOSFIT program, Maine University, France."

[38] Larson A. C. and R. B. von Dreele, *General Structure Analysis System (GSAS)*. Los Alamos National Laboratory Report LAUR, 2004.

[39] J. Gao, T. Volkmann, S. Roth, W. Löser, and D. M. Herlach, "Phase formation in undercooled NdFeB alloy droplets," *Journal of Magnetism and Magnetic Materials*, vol. 234, no. 2, 2001, doi: 10.1016/S0304-8853(01)00388-2.

[40] S. C. Wang and Y. Li, "A new structure of Nd1+εFe4B4 phase in NdFeB magnet," *Journal of Materials Science*, vol. 40, no. 14. 2005, doi: 10.1007/s10853-005-2554-y.

[41] S. Gang, H. Lianxi, and W. Erde, "Preparation, microstructure, and magnetic properties of a nanocrystalline Nd12Fe82B6 alloy by HDDR combined with mechanical milling," *Journal of Magnetism and Magnetic Materials*, vol. 301, no. 2, 2006, doi: 10.1016/j.jmmm.2005.07.015.

[42] H. chao Sheng, X. rong Zeng, D. ju Fu, and F. Deng, "Differences in microstructure and magnetic properties between directly-quenched and optimally-annealed Nd-Fe-B nanocomposite materials," *Physica B: Condensed Matter*, vol. 405, no. 2, 2010, doi: 10.1016/j.physb.2009.09.088.

[43] G. C. Hadjipanayis and W. Gong, "Magnetic hysteresis in melt-spun Nd-Fe-Al-B-Si alloys with high remanence," *Journal of Applied Physics*, vol. 64, no. 10, 1988, doi: 10.1063/1.342307.

[44] A. Manaf, R. A. Buckley, and H. A. Davies, "New nanocrystalline high-remanence Nd-Fe-B alloys by rapid solidification," *Journal of Magnetism and Magnetic Materials*, vol. 128, no. 3, 1993, doi: 10.1016/0304-8853(93)90475-H.

[45] F. Bolzoni, J. P. Gavigan, D. Givord, H. S. Li, O. Moze, and L. Pareti, "3d magnetism in R2Fe14B compounds," *Journal of Magnetism and Magnetic Materials*, vol. 66, no. 1, 1987, doi: 10.1016/0304-8853(87)90139-9.

[46] M. Sagawa, S. Hirosawa, H. Yamamoto, S. Fujimura, and Y. Matsuura, "Nd卌fe卌b permanent magnet materials," *Japanese Journal of Applied Physics*, vol. 26, no. 6R, 1987, doi: 10.1143/JJAP.26.785.

[47] J. S. T. Hernández, J. A. Tabares, and G. A. P. Alcázar, "Structural, magnetic, and mechanical hardness characterization of the alloy Nd16(Fe76−xNix)B8 with x = 0, 10, 20, and 25," *Applied Physics A: Materials Science and Processing*, vol. 124, no. 10, 2018, doi: 10.1007/s00339-018-2119-y.

[48] S. Dai, A. H. Morrish, X. Z. Zhou, B. P. Hu, and S. G. Zhang, "Mössbauer study of the permanent-magnet material Nd 2(Fe1-xNix)14B," *Journal of Applied Physics*, vol. 63, no. 8, 1988, doi: 10.1063/1.340647.

[49] L. X. Liao, Z. Altounian, and D. H. Ryan, "Cobalt site preferences in iron rare-earth-based compounds," *Physical Review B*, vol. 47, no. 17, 1993, doi: 10.1103/PhysRevB.47.11230.

[50] C. Lin, Z. X. Liu, Y. X. Sun, C. X. Bai, and T. S. Zhao, "Effect of exchange interaction on spin reorientation in the Nd2Fe14B system," *Physical Review B*, vol. 39, no. 10, 1989, doi: 10.1103/PhysRevB.39.7273.